13. Lacin, H., and Truman, J.W. (2016). Lineage mapping identifies molecular and architectural similarities between the larval and adult Drosophila central nervous system. eLife *5*, e13399.

14. Bizzi, E., Giszter, S.F., Loeb, E., Mussa-Ivaldi, F.A., and Saltiel, P. (1995). Modular organization of motor behavior in the frog's spinal cord. Trends Neurosci. *18*, 442–446.

15. Büschges, A., and Ache, J.M. (2025). Motor control on the move: from insights in insects to general mechanisms. Physiol. Rev. *105*, 975–1031.

16. Grillner, S. (2023). The Brain in Motion (The MIT Press), https://doi.org/10.7551/mitpress/14411.001.0001.

17. Vandervorst, P., and Ghysen, A. (1980). Genetic control of sensory connections in Drosophila. Nature *286*, 65–67.

18. Kupfermann, I., and Weiss, K.R. (1978). The command neuron concept. Behav. Brain Sci. *1*, 3–10.

19. Berg, E.M., Hooper, S.L., Schmidt, J., and Büschges, A. (2015). A leg-local neural mechanism mediates the decision to search in stick insects. Curr. Biol. *25*, 2012–2017.

20. Marin, E.C., Morris, B.J., Stürner, T., Champion, A.S., Krzeminski, D., Badalamente, G., Gkantia, M., Dunne, C.R., Eichler, K., Takemura, S.-Y., *et al*. (2024). Systematic annotation of a complete adult male Drosophila nerve cord connectome reveals principles of functional organisation. eLife *13*, RP97766. https://doi.org/10.7554/elife.97766.1.

# Touch sensation: Convergent mechanical sensitivity between elephant and rat whiskers

**Rishyashring R. Iyer[1], Arash Fassihi[1], Hyein Park[1], Pantong Yao[2], David Kleinfeld[1,3,*], and David Golomb[4,5,*]**
[1]Department of Physics, University of California at San Diego, La Jolla, CA 92093, USA
[2]Neurosciences Graduate Program, University of California at San Diego, La Jolla, CA 92093, USA
[3]Department of Neurobiology, University of California at San Diego, La Jolla, CA 92093, USA
[4]Department of Physiology and Cell Biology, Ben Gurion University, Be'er-Sheva 8410501, Israel
[5]Zelman Center for Brain Sciences, Ben Gurion University, Be'er-Sheva 8410501, Israel
*Correspondence: dk@physics.ucsd.edu (D.K.), golomb@bgu.ac.il (D.G.)
https://doi.org/10.1016/j.cub.2026.04.001

**New work reveals that elephant whiskers, also known as vibrissae, have elliptical, stiff, and porous bases along with soft tips. This contrasts with the uniform, highly tapered nature of rodent vibrissae. Nonetheless, these differences in design lead to similar mechanical sensitivity to vibrissa-based touch.**

Touch at a distance, which animals perform through long, inert hairs called vibrissae or whiskers, provides a measure of safety, efficiency, and even improved spatial resolution compared to touch directly on the skin. The stem group for Mammaliaformes developed the genetic underpinnings and the skull structure for facial vibrissae in the middle Triassic period (~240 Mya). Despite having diverged from the early placental mammals along the phylogenetic tree approximately 100 Mya, and notwithstanding a more than 10,000-fold difference in their body volumes, elephants and rats have vibrissae of approximately similar length (Figure 1A). To navigate within their natural habitats of narrow underground burrows, rodents actively and rhythmically palpate with their vibrissae to identify the texture of their surroundings and localize objects within a few centimeters' reach of the vibrissae[1–4]. Most other mammals, including non-human primates, have passive vibrissa systems adapted for different needs of tactile interactions with their environments. Seals use vibrissa to detect minute water movements[5] because visual and auditory information can be unreliable underwater. Nocturnal animals such as cats use their vibrissae to detect objects at short range and navigate in low-light conditions. It is reasonable to conjecture that elephants use their vibrissa, which lie along the posterior and lateral sides of their trunks, to detect surfaces as they actively contort and sway their trunks.

A recent article[6] published in *Science* from Katherine Kuchenbecker's group reports on the morphology and mechanics of elephant vibrissae and highlights how material properties influence tactile sensitivity and endurance. In gross form, elephant vibrissae have a substantially smaller geometric taper for their length compared to the popularly studied vibrissae from rodents[7] and even seals[5] (Figure 1B). Kuchenbecker's group probed the value and spatial distribution of four material properties of vibrissae originating at the distal end of the trunk of Asian elephants (Figure 1C). They report on: porosity along the shaft, as measured using scanning electron microscopy (SEM) and computed x-ray tomography; elasticity, as quantified by Young's modulus and probed by nanoindentation; geometric taper, as measured using SEM; and circular through elliptical cross-sections from the base to the tip of the vibrissa, as measured using SEM. These authors concluded that elephant vibrissae have: an 80% porous base, with hollow channels that span halfway up the length of the vibrissa; a stiff base and a soft tip, where the Young's modulus at the tip is 100-fold smaller than at the base; a geometric taper where the radius of the base is threefold greater than that at the tip; and cross-sections that vary from circular to elliptical, where the ratio of the major and minor axes varies from 1:1 to

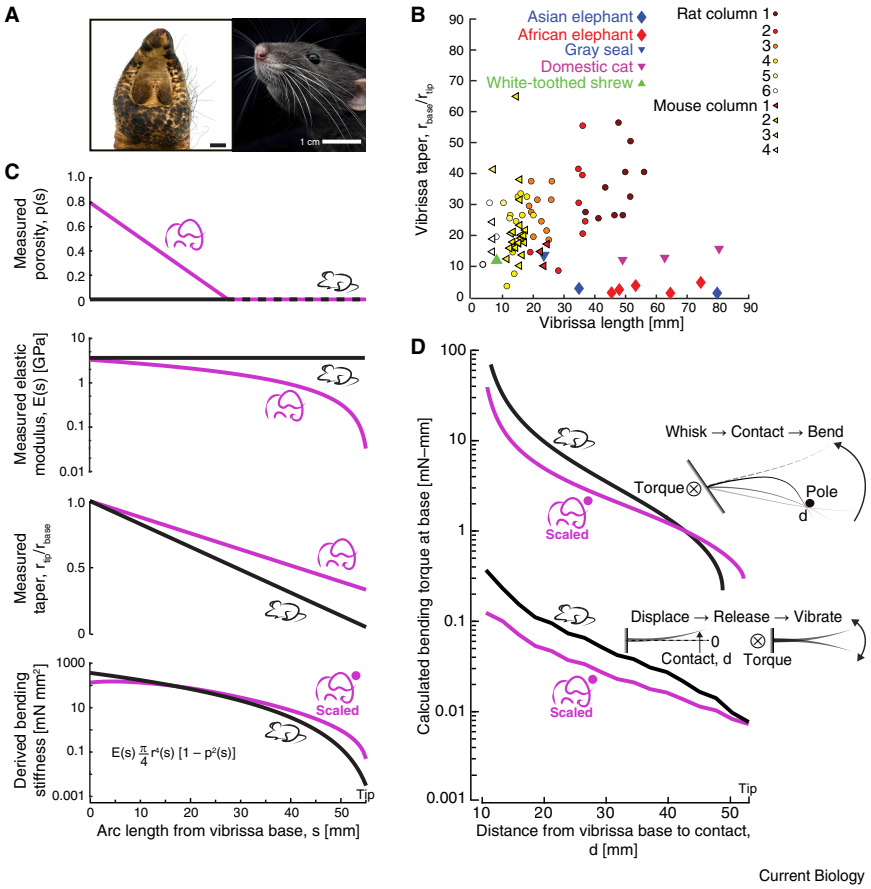


**Figure 1. Material and morphometric properties of different vibrissae and their response to touch.**

(A) Images of vibrissae. (Left) Tip of an Asian elephant's trunk and (right) the mystacial pad of a rat. Trunk image reused from[15] and rat image reused from[9] (CC BY 4.0). (B) Relationship between taper ratio and vibrissa length across species. Scatter plot of taper ratio ($r_{base}/r_{tip}$) as a function of vibrissa length. Data from mice (triangles)[16] and rats (circles)[17] are color-coded by whisker columns (inset). Additional species are overlaid for comparison: Asian elephant (blue diamond)[6], African elephant (red diamond)[15], gray seal (blue triangle)[18], white-toothed shrew (green triangle)[19], and the domestic cat (magenta triangle)[20]. (C) Mechanical properties of vibrissae from rat (black) and elephant (purple). From top to bottom: porosity, p(s), which is a function of arc length s along the vibrissa shaft and is variable for elephant vibrissae but is constant for rat vibrissae; Young's modulus, E(s), which is variable for elephant vibrissae but is constant for rat vibrissae; vibrissa radius, r(s), which is 'exact' for the rat but scaled for the elephant so that the rat and the elephant have the same radius at their base, yet we respect the difference in taper (approximately 19:1 for rat and 3:1 for elephant). The stiffness is derived as $E(s)I_a(s)$. The area moment of inertia $I_a(s)$ is calculated assuming that a vibrissa cross-section is equivalent to that of a pipe with outer and inner radii of r and $r_{in}$, respectively, where the inner radius is $r_{in} = r\sqrt{p}$ and $I_a(s) = (\pi/4)(r^4 - r_{in}^4)$[12]. Porosity is incorporated through the equivalent hollow rod. All vibrissae lengths are 53 mm, $r_{base}$ = 105 μm and $r_{tip}$ = 5.5 μm for the rat, and $r_{base}$ = 105 μm and $r_{tip}$ = 35 μm for the scaled elephant. (D) The bending torque for mechanical activation of rat and scaled elephant vibrissae is pushed into a pole for the rat, elephant, and scaled elephant vibrissae. For contact with a pole, the vibrissa is pushed with an angle at the base of 10° into a pole with radius of 250 μm. The torque is plotted as a function of the distance (d) between the vibrissa base and the center of the pole. The distance d and the arc length s are related[13]. The lines end when d is smaller than the vibrissa length, s, because of slip-off. For transformation of vibration at the tip to a torque at the base, the bending torque is estimated from dynamic finite element analysis (FEA) in response to a momentary displacement of 100 μm at a location from the base, s, where s = d for the assumed straight vibrissa, at time t = 0, followed by free vibration. The FEA model, written in Abaqus and executed using Abaqus2Matlab, was adapted from Schulz *et al.*[6], where the undulations in the reaction force are expressed as the sum of sinusoids of unique eigenmodes.

3:1 across the ensemble of elephant vibrissae. In contrast, vibrissae from rodents are highly tapered, with roughly a 20:1 difference in radius from base to tip, and have an almost-conical shape[8] (Figure 1C). Taken together, Kuchenbecker's measurements of these quantities[6], which were also performed for mouse vibrissae, set the stage for a mechanics-based analysis of the relative stiffness and bending moment of elephant versus murine vibrissae.

The vibrissae of the Asian elephant differ in material and dimensional properties from those of the rat (Figure 1C). Yet, only the amalgam of physical parameters is important to determine the sensitivity to distant touch. A derived quantity that underlies all mechanical measures of sensitivity is the bending stiffness of the vibrissa, which will vary along the length of the shaft. Stiffness determines the resistance to bending and depends on radius, porosity, and Young's elastic modulus (Figure 1C). Here we set out to evaluate the comparative stiffness between rat and elephant vibrissae, taking both vibrissae to have the same length, which is close to the natural case, and a circular cross-section. As the elephant vibrissa is 10-fold thicker at the base, we scale the radius of the elephant vibrissa to have the same thickness at the base as that of the rat vibrissa. The profiles of porosity, elastic modulus, and taper were unchanged (Figure 1C), so that the comparison is between two vibrissae of the same length and thickness at the base but realized with different material and dimensional properties. It is remarkable that the derived values for the stiffness of the scaled-elephant and the rat vibrissae are close or overlapping in value along essentially the entire length of their shafts (Figure 1C). This convergence to a similar profile of stiffness versus position shows that mechanical differences in materials between elephant and rat vibrissae are offset by differences in the gradient of material properties and the taper of the vibrissae. For the elephant vibrissa, the gradient in porosity counteracts the gradient in elastic modulus and leads to smaller stiffness at the base. Furthermore, the gradient in elasticity also compensates for the lack of taper and leads to a reduced stiffness at the tip. For the rat vibrissa, the greater geometric taper drives the decrease in stiffness from base to tip.

We then calculated the reaction torque of the vibrissae to distant touch at different locations along the shaft. The reaction forces induced by this torque are sensed by mechanosensory neurons within the follicle[9,10] and drive spiking by

trigeminal sensory neurons[11]. The reaction torque was evaluated in two ways (Figure 1D). The first, a quasi-static approach, assumed that the vibrissae reached a steady-state position at every instant following contact, where bending during contact causes the base of the vibrissae to slowly move and rotate[12]. The estimated reaction torques from the scaled-elephant and rat vibrissae are close, within a factor of two, for contact at all locations along the shaft except the tip (Figure 1D). This analysis also demonstrates that the vibrissa will slip off the object before the contact point reaches the tip or full length of the vibrissa. Slip-off occurs for more proximal objects with the highly tapered rat vibrissa, which is particularly effective in producing stick–slip events that are essential for texture characterization[13,14]. The second analysis, a dynamic approach, evaluated the transformation of the natural vibration of the tip to a vibratory reaction torque at the base. Here the scaled-elephant vibrissa had roughly a twofold lower torque at the base compared to that of the rat vibrissa (Figure 1D). The elasticity gradient increased the difference in amplitude of the vibrations when contacted at different positions along the vibrissa shaft, improving the gradient in sensitivity so that rat and elephant vibrissae had equal reaction torques at their tips (Figure 1D). All told, these results support convergent evolution to a common mechanical sensitivity to distant touch.

For the 'real', full-size elephant vibrissa, the reaction torque at the base is more than 100-fold greater in both quasi-static and dynamic analyses. Nonetheless, the slope of the reaction force versus contact position remains the same as that for a scaled-elephant vibrissa, suggesting that the sensitivity is dominated by the relative gradients in geometry and elasticity as opposed to absolute size. Further, while the reaction force from ellipsoidal vibrissae contacted at the horizontal versus vertical orientation creates a 10-fold difference in the value of the reaction torque at the base, the fractional sensitivity to a change in reaction torque along the shaft is the same for horizontally oriented ellipsoidal, vertically oriented ellipsoidal, and round vibrissae. Thus, the ellipsoidal feature of elephant vibrissae appears not to aid in discrimination by distant touch.

Parallel evolution in the design of the elephant and the rat vibrissae may optimize for more than sensitivity to touch. First, while most mammals regrow their vibrissae robustly after loss, elephant vibrissae do not regrow[15]. Second, whereas active sensing in elephants does not involve active whisking of individual vibrissae, elephant vibrissae operate as passive tactile sensors embedded within a highly flexible and mobile trunk and encounter forces that are orders of magnitude larger than the forces encountered by rodent vibrissae. Thus, the low taper, elliptical shape, and high porosity at the base, which decreases the sensitivity to touch, could have developed for improving the resistance of elephant vibrissae to wear and loss. What makes elephant vibrissae remarkable is that an elastic gradient compensates for the lack of taper in the scaled vibrissae and that ellipticity does not affect the ratio of torques in the analysis of distant touch. All told, the new precision measurements[6] (Figure 1C) and analysis (Figure 1C,D) highlight how the material and morphological properties of vibrissae from disparate species provide insight into nature's design of appendages to sense distant touch.

## DECLARATION OF INTERESTS

The authors declare no competing interests.

## REFERENCES

1. Mitchinson, B., Grant, R.A., Arkley, K., Rankov, V., Perkn, I., and Prescott, T.J. (2011). Active vibrissal sensing in rodents and marsupials. Philos. Trans. R. Soc. Lond. B Biol. Sci. *366*, 3037–3048.
2. Bush, N.E., Solla, S.A., and Hartmann, M.J.Z. (2016). Whisking mechanics and active sensing. Curr. Opin. Neurobiol. *40*, 178–188.
3. Sofroniew, N.J., and Svoboda, K. (2015). Whisking. Curr. Biol. *25*, R137–R140.
4. Kleinfeld, D., and Deschênes, M. (2011). Neuronal basis for object location in the vibrissa scanning sensorimotor system. Neuron *72*, 455–468.
5. Dehnhardt, G., Mauck, B., and Bleckmann, H. (1998). Seal whiskers detect water movements. Science *394*, 235–236.
6. Schulz, A.K., Kaufmann, L.V., Smith, L.T., Philip, D.S., David, H., Lazovic, J., Brecht, M., Richter, G., and Kuchenbecker, K.J. (2026). Functional gradients facilitate tactile sensing in elephant whiskers. Science *391*, 712–718.
7. Chernova, O.F., and Zherebtsova, O.V. (2023). Architecture of vibrissae in eight rodent species of Ctenohystrica (Rodentia): A comparative SEM study. Zool. Anz. *307*, 54–69.
8. Quist, B.W., and Hartmann, M.J.Z. (2012). Mechanical signals at the base of a rat vibrissa: The effect of intrinsic vibrissa curvature and implications for tactile exploration. J. Neurophysiol. *107*, 2298–2312.
9. Muramoto, T., Furuta, T., Koike, T., Bagdasarian, K., Tonomura, S., Takenaka, A., Kataoka, Y., Maeda, M., Eguchi, A., Kitada, M., *et al*. (2025). Club-like receptors respond to light touch but not to whisking. Nat. Commun. *16*, e11343.
10. Whiteley, S.J., Knutsen, P.M., Matthews, D.M., and Kleinfeld, D. (2015). Deflection of a vibrissa leads to a gradient of strain across mechanoreceptors in the mystacial follicle. J. Neurophysiol. *114*, 138–145.
11. Severson, K.S., Xu, D., Van de Loo, M., Bai, L., Ginty, D.D., and O'Connor, D.H. (2017). Active touch and self-motion encoding by Merkel cell-associated afferents. Neuron *94*, 666–676.
12. Birdwell, J.A., Solomon, J.H., Thajchayapong, M., Taylor, M.A., Cheely, M., Towal, R.B., Conradt, J., and Hartmann, M.J. (2007). Biomechanical models for radial distance determination by the rat vibrissal system. J. Neurophysiol. *98*, 2439–2455.
13. Hires, S.A., Pammer, L., Svoboda, K., and Golomb, D. (2013). Tapered whiskers are required for active tactile sensation. eLife *2*, e01350.
14. Ding, Y., and Vlasov, Y. (2023). Pre-neuronal processing of haptic sensory cues via dispersive high-frequency vibrational modes. Sci. Rep. *13*, e14370.
15. Deiringer, N., Schneeweiß, U., Kaufmann, L.V., Eigen, L., Speissegger, C., Gerhardt, B., Holtze, S., Fritsch, G., Göritz, F., Becker, R., *et al*. (2023). The functional anatomy of elephant trunk whiskers. Commun. Biol. *6*, e591.
16. Hires, S.A., Schuyler, A., Sy, J., Huang, V., Wyche, I., Wang, X., and Golomb, D. (2016). Beyond cones: An improved model of whisker bending based on measured mechanics and tapering. J. Neurophysiol. *116*, 812–824.
17. Belli, H.M., Callister, R.J., and Peterson, E.H. (2017). Variations in vibrissal geometry across the rat mystacial pad: Base diameter, medulla, and taper. J. Neurophysiol. *117*, 1807–1820.
18. Zheng, X., Kamat, A.M., Cao, M., Triantafyllou, M.S., and Kottapalli, A.G.P. (2025). Wonders of harbor and grey seal whiskers: Morphology, natural frequencies, and 3D modeling. Adv. Sci. *12*, e2500724.
19. Dougill, G., Starostin, E.L., Milne, A.O., van der Heijden, G.H.M., Goss, V.G.A., and Grant, R.A. (2020). Ecomorphology reveals Euler spiral of mammalian whiskers. J. Morphol. *281*, 1271–1279.
20. Dougill, G., Brassey, C.A., Starostin, E.L., Andrews, H., Kitchener, A., van der Heijden, G.H.M., Gross, V.G.A., and Grant, R.A. (2023). Describing whisker morphology of the Carnivora. J. Morphol. *284*, e21628.